

NIMROD: properties to consider for code integration

C. R. Sovinec

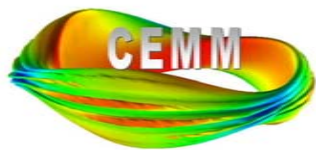
University of Wisconsin-Madison

for the NIMROD Team

Workshop on Computational Frameworks in Fusion

Oak Ridge National Laboratory

January 29-31, 2007



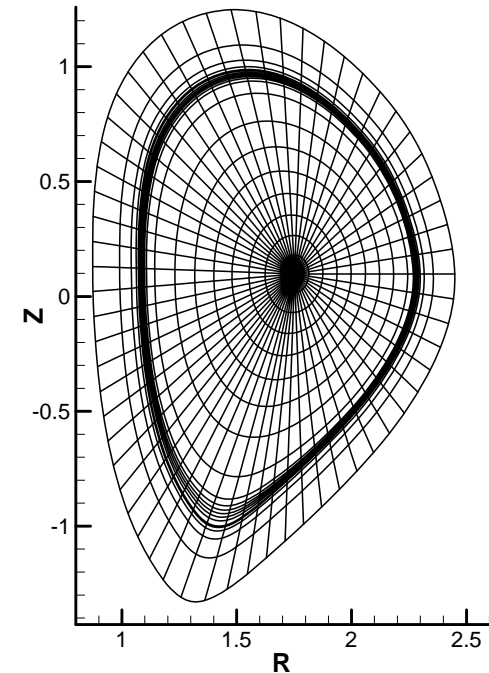
Thesis and Outline

The NIMROD code is an excellent candidate for macroscopic dynamics in integrated modeling efforts; it is mature but still actively developed. Its spatial representation and data structures are the most significant aspects for code integration.

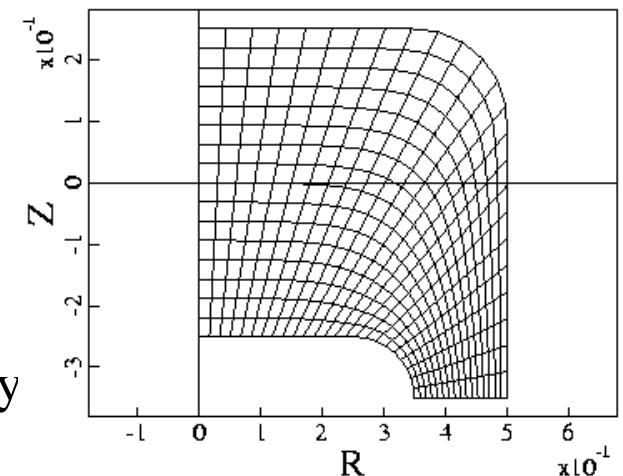
- Introduction
- NIMROD's internal 'framework'
- Time-advance information
- Highlights from recent code development
 - Parallel kinetics
 - Two-fluid modeling
- Coupling with RF for 'slow' MHD
- Discussion

Introduction: what is NIMROD?

- NIMROD is an extended-MHD code for macroscopic plasma dynamics.
 - Low frequency--well below electron dynamics
 - Large wavelength--global domain
 - Full magnetic evolution and topology change
- Geometry is sufficiently general to require something of a framework.
 - Cross section shape is arbitrary--blocks of 2D finite elements (arbitrary order--technically spectral).
 - At least one coordinate is periodic--Fourier representation.
 - Domain cross section is uniform in periodic coordinate--mapping is limited to being independent of this coordinate.
- Stiffness requires implicit methods, but it is relatively easy to change how the fields are advanced.



Mesh for ELM computations.



Mesh for SSPX simulation.

What NIMROD solves: fluid-moment evolution equations and Maxwell's equations are the basis of our extended-MHD system.

$$\frac{\partial \mathbf{B}}{\partial t} = -\nabla \times \left(\eta \mathbf{J} - \mathbf{V} \times \mathbf{B} + \frac{1}{ne} \mathbf{J} \times \mathbf{B} - \frac{T_e}{ne} \nabla n \right) + \kappa_{divb} \nabla \nabla \cdot \mathbf{B}$$

Faraday's / Ohm's law

$$\mu_0 \mathbf{J} = \nabla \times \mathbf{B}$$

low- ω Ampere's law

$$\rho \left(\frac{\partial \mathbf{V}}{\partial t} + \mathbf{V} \cdot \nabla \mathbf{V} \right) = \mathbf{J} \times \mathbf{B} - \nabla p - \nabla \cdot \Pi_i(\mathbf{V})$$

flow evolution

$$\frac{\partial n}{\partial t} + \nabla \cdot (n \mathbf{V}) = \nabla \cdot D \nabla n$$

particle continuity
with artificial diffusivity

$$\frac{n}{\gamma - 1} \left(\frac{\partial T_\alpha}{\partial t} + \mathbf{V}_\alpha \cdot \nabla T_\alpha \right) = -p_\alpha \nabla \cdot \mathbf{V}_\alpha - \nabla \cdot \mathbf{q}_\alpha + Q_\alpha$$

temperature evolution

- The magnetic divergence term and particle diffusion term are used for numerical purposes.
- Quasineutrality is assumed.

The relations used for \mathbf{E} , Π , and \mathbf{q}_α determine which theoretical model is solved. [resistive MHD, two-fluid, kinetic effects, etc.]

- Collisional closure relations have limited applicability, but they provide dissipation that is necessary for nonlinear simulations if the algorithm is not inherently dissipative.

Π_i is a combination of Π_{gv} , Π_{\parallel} , and Π_{\perp}

$$\Pi_{\text{gv}} = \frac{m_i p_i}{4eB} \left[\hat{\mathbf{b}} \times \mathbf{W} \cdot (\mathbf{I} + 3\hat{\mathbf{b}}\hat{\mathbf{b}}) - (\mathbf{I} + 3\hat{\mathbf{b}}\hat{\mathbf{b}}) \cdot \mathbf{W} \times \hat{\mathbf{b}} \right], \quad \left(\mathbf{W} \equiv \nabla \mathbf{V} + \nabla \mathbf{V}^T - \frac{2}{3} \mathbf{I} \nabla \cdot \mathbf{V} \right)$$

$$\Pi_{\parallel} = \frac{p_i \tau_i}{2} (\hat{\mathbf{b}} \cdot \mathbf{W} \cdot \hat{\mathbf{b}}) (\mathbf{I} - 3\hat{\mathbf{b}}\hat{\mathbf{b}})$$

$$\Pi_{\perp} \sim -\frac{3p_i m_i^2}{10e^2 B^2 \tau_i} \mathbf{W} \text{ has been treated as } -nm_i v_{iso} \mathbf{W} \text{ or } -nm_i v_{kin} \nabla \mathbf{V}$$

$$\mathbf{q}_i = -n \left[\chi_{\parallel i} \hat{\mathbf{b}}\hat{\mathbf{b}} + \chi_{\perp i} (\mathbf{I} - \hat{\mathbf{b}}\hat{\mathbf{b}}) \right] \cdot \nabla T_i + 2.5 p_i (eB)^{-1} \hat{\mathbf{b}} \times \nabla T_i$$

$$\mathbf{q}_e = -n \left[\chi_{\parallel e} \hat{\mathbf{b}}\hat{\mathbf{b}} + \chi_{\perp e} (\mathbf{I} - \hat{\mathbf{b}}\hat{\mathbf{b}}) \right] \cdot \nabla T_e - 2.5 p_e (eB)^{-1} \hat{\mathbf{b}} \times \nabla T_e$$

- Closure terms with local gradients may be treated implicitly and can be used in semi-implicit advances with nonlocal closures. [Held, PoP **11**, 2419 (2004)]
- Most computations to date use a single temperature.

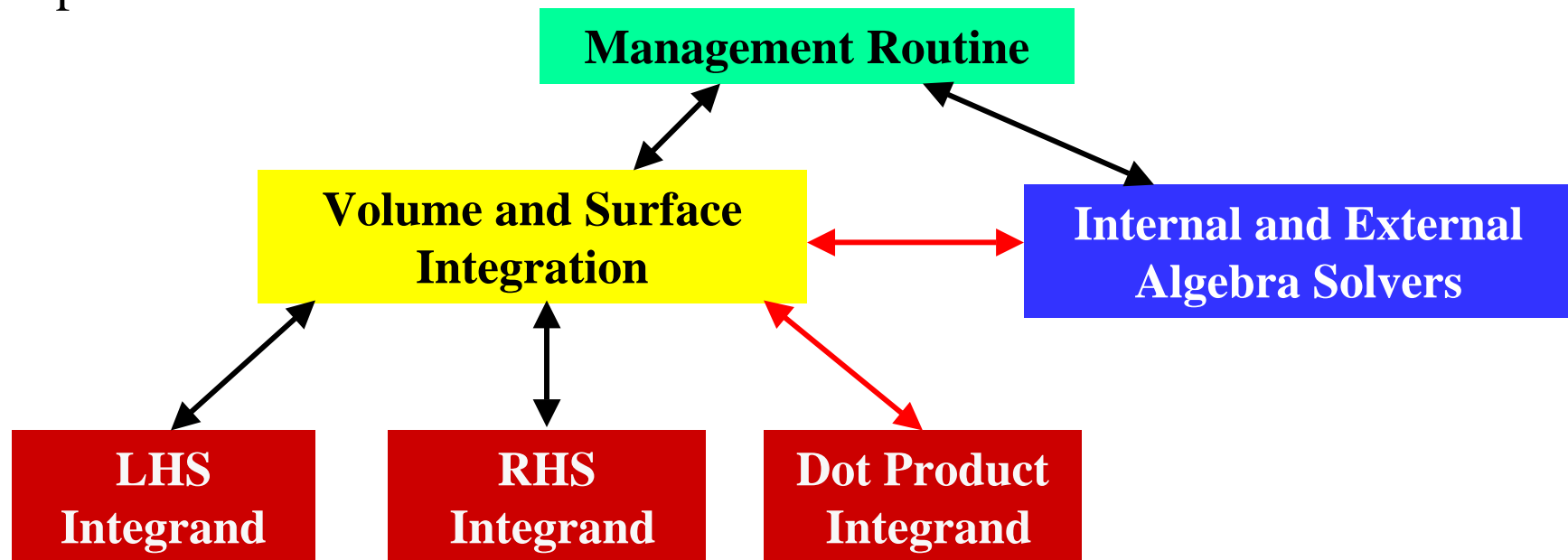
Where NIMROD is used: the list of current applications shows that it gets a lot of exercise on production problems.

1. *Astrophysical jet configurations*, C. Cary
2. *Ballooning instability in the magnetotail*, P. Zhu
3. *CDX-U sawteeth & related*, S. Kruger, J. O'Bryan, D. Schnack, C. Sovinec
4. *Disruption mitigation in tokamaks*, V. Izzo
5. *Edge Localized Modes*, D. Brennan, S. Kruger, C. Sovinec
6. *ELM modeling for ITER*, A. Pankin
7. *Energetic particles in RFP tearing modes*, C. Kim
8. *Helicity injection for STs*, A. Bayliss
9. *HIT-SI*, C. Akcay
10. *Kinetic heat flux in SSPX*, E. Held, J.-Y. Ji
11. *Modeling of the Caltech jet experiment*, C. Kim
12. *Nonlinear evolution and linear modes in SSPX*, B. Cohen, B. Hooper, E. Howell, L. Lodestro
13. *Plasma thruster*, A. Tarditi
14. *Pulsed poloidal current drive in RFPs*, J. Reynolds
15. *Resistive wall machine studies*, C. Cary, C. Sovinec
16. *Two-fluid FRC studies*, D. Barnes, A. MacNab, and R. Milroy
17. *Two-fluid reconnection in MRX and SSX*, N. Murphy
18. *Two-fluid RFP dynamo*, J. King

NIMROD's Internal Framework

Though usually used for one purpose, NIMROD itself is a PDE solver.

- The present time-advance has independent solves for different fields.
- Each advance uses the same software machinery for the FE/spectral representation.



- Physics is installed at the integrand level.
- Connections in red arise from matrix-free algebra.

Data is organized by grid 'block' (or subdomain) and sliced into layers of Fourier components.

- There are arrays of F90 structures of blocks which hold basis-function information for interpolation.
 - Structured, arbitrary-order quadrilaterals
 - Unstructured linear triangles
 - Others are possible in principle
- Memory for coefficients of the expansions is allocated in structures contained in these blocks.
 - Basis-function information is evaluated at the volume- and surface-integration level.
 - Integrand (physics) routines are independent of block-type.
- Arrays of structures holding pointer arrays provide access to coefficients, independent of the type of block.
 - This information is used at the management-level and is sent to algebra-solver routines.
 - Most parallel communication among blocks is local point-to-point.
- Operations that couple different Fourier components apply FFTs and require communication that is global within communicator-sets.

Time-advance Information

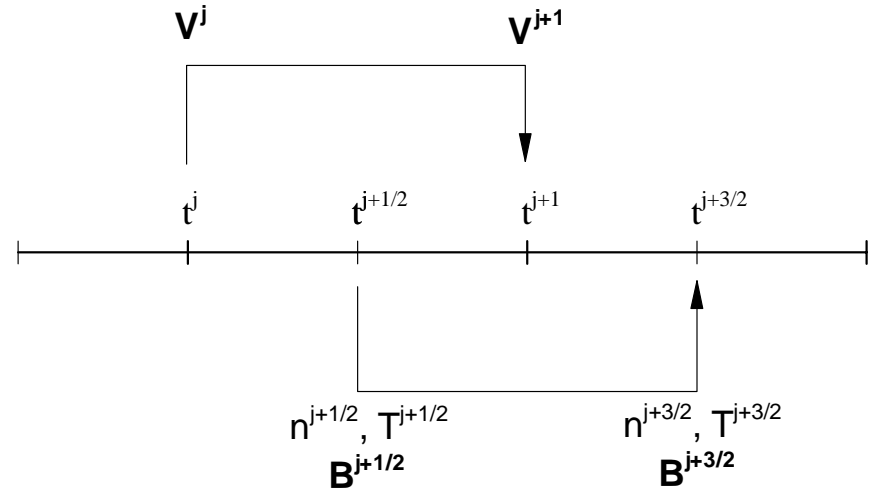
The NIMROD algorithm staggers different fields in time.

Neglecting advection, dissipation, and the separate n and T advances for clarity:

$$(\rho + \Delta t^2 L) \Delta \mathbf{V} = (\Delta t \mathbf{J}^{n+1/2} \times \mathbf{B}^{n+1/2} - \Delta t \nabla p^{n+1/2})$$

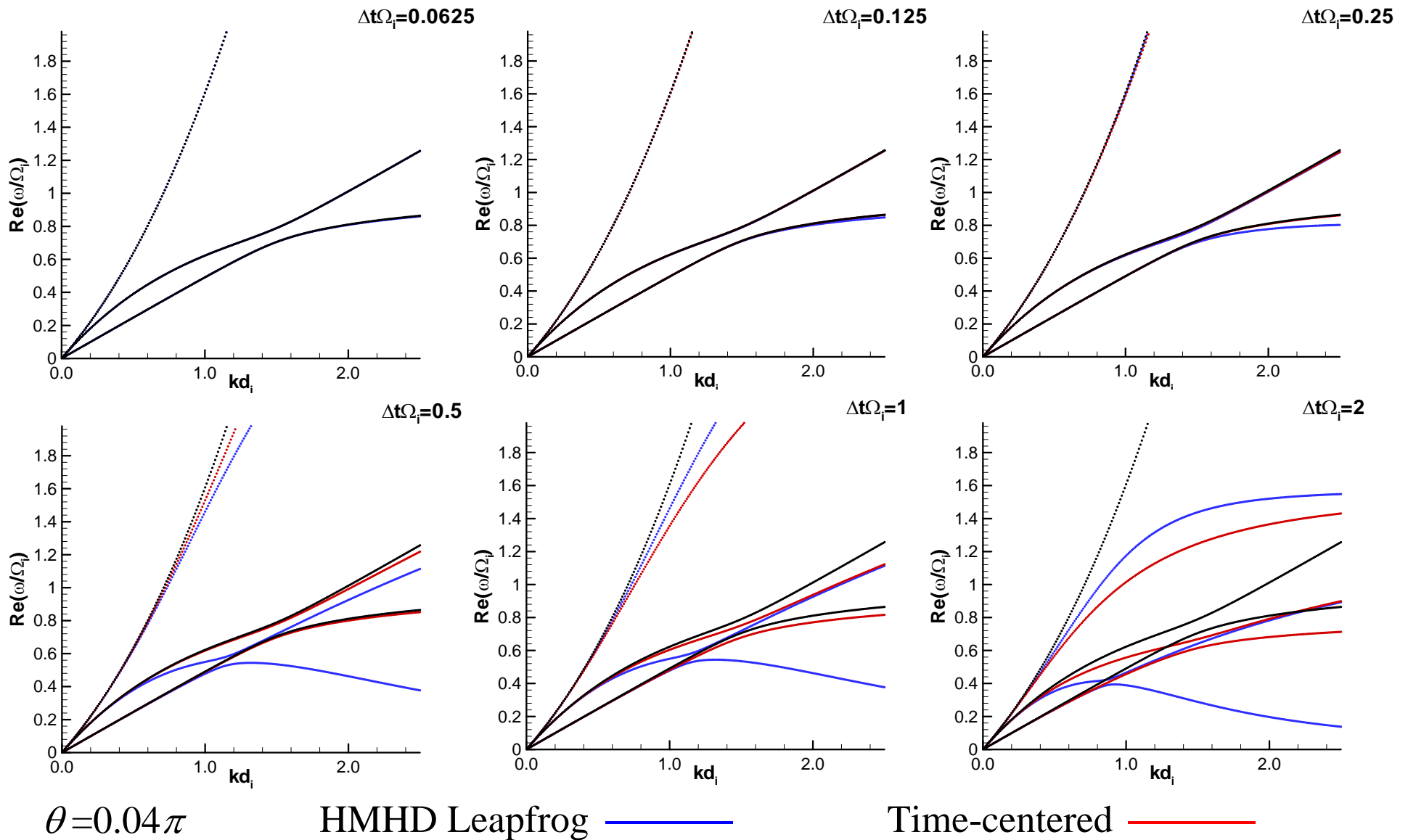
$$\Delta p + \frac{\Delta t}{2} \gamma \Delta p \nabla \cdot \mathbf{V}^{n+1} = -\Delta t \gamma p^{n+1/2} \nabla \cdot \mathbf{V}^{n+1}$$

$$\Delta \mathbf{B} + \frac{\Delta t}{2} \nabla \times \frac{1}{ne} \left(\mathbf{J}^{n+1/2} \times \Delta \mathbf{B} + \frac{\nabla \times \Delta \mathbf{B}}{\mu_0} \times \mathbf{B}^{n+1/2} \right) = \Delta t \nabla \times (\mathbf{V}^{n+1} \times \mathbf{B}^{n+1/2}) - \Delta t \nabla \times \frac{1}{ne} (\mathbf{J}^{n+1/2} \times \mathbf{B}^{n+1/2} - \nabla p_e)$$

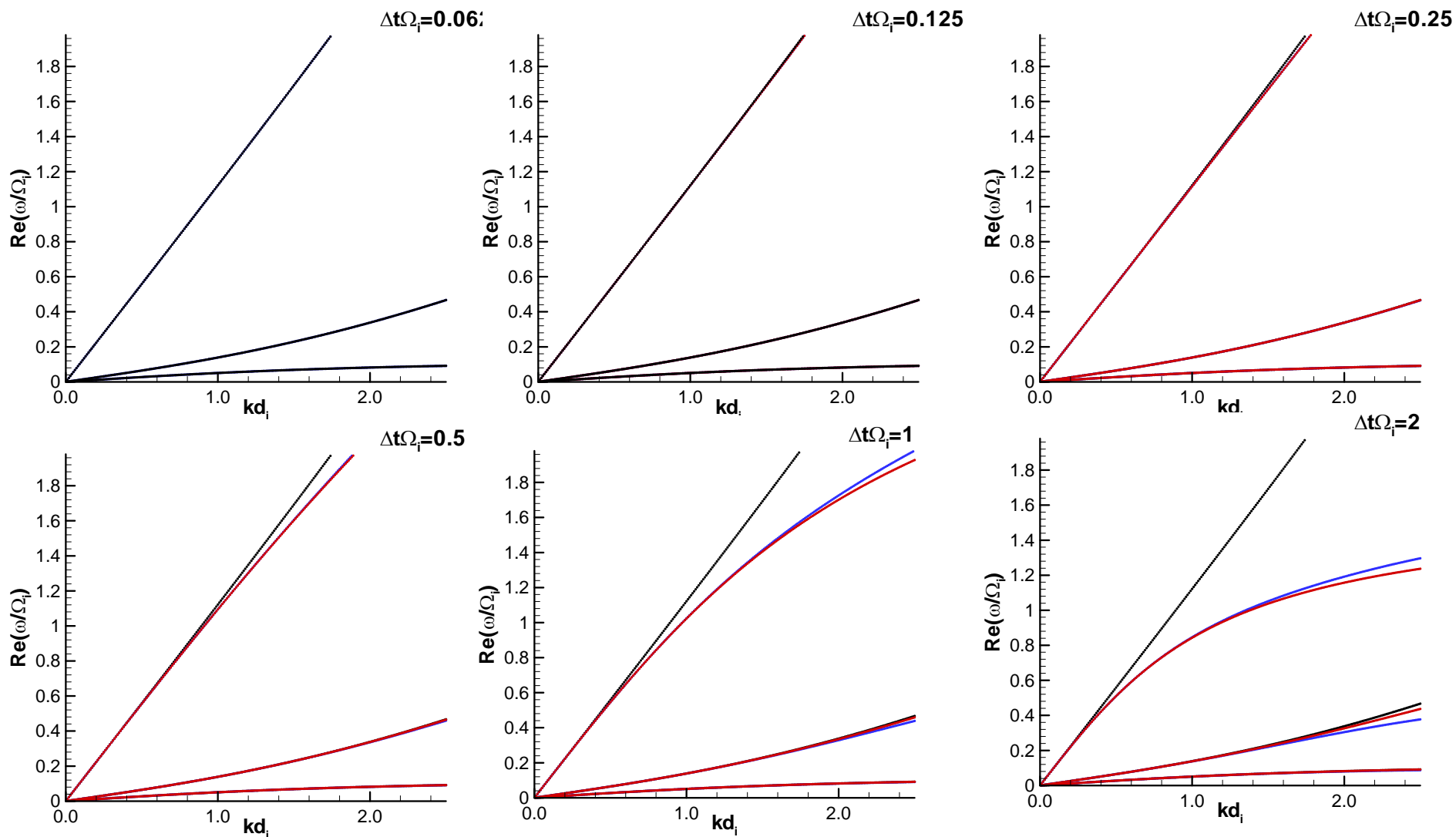


- The implicit Hall terms are linearized from the beginning of a time-step, resulting in second-order differential operators that are not self-adjoint.
- The advantage over full implicit time-centering is that the resulting algebraic systems are smaller.

Comparing IL with time-centered, IL shows more numerical dispersion in the cyclotron resonance and slightly less in the whistler for $\Delta t \Omega_i > 0.5$.



There is less to distinguish the two algorithms for nearly perpendicular propagation, except that time-centered has better accuracy for the KAW.



$\theta = 0.46\pi$

HMHD Leapfrog ————

Time-centered ————

Treatment of externally generated ‘equilibria’ is an important subtlety.

- For accuracy [Popov, et al., PoP **8**, 3605 (2001)], NIMROD is written to solve the nonlinear distortion from a steady state.

- For example, Faraday’s law for resistive MHD appears as

$$\frac{\partial \mathbf{b}}{\partial t} = \nabla \times (\mathbf{V}_0 \times \mathbf{b} + \mathbf{v} \times \mathbf{B}_0 + \mathbf{v} \times \mathbf{b} - \eta_0 \mathbf{j} - \tilde{\eta} \mathbf{J}_0 - \tilde{\eta} \mathbf{j})$$

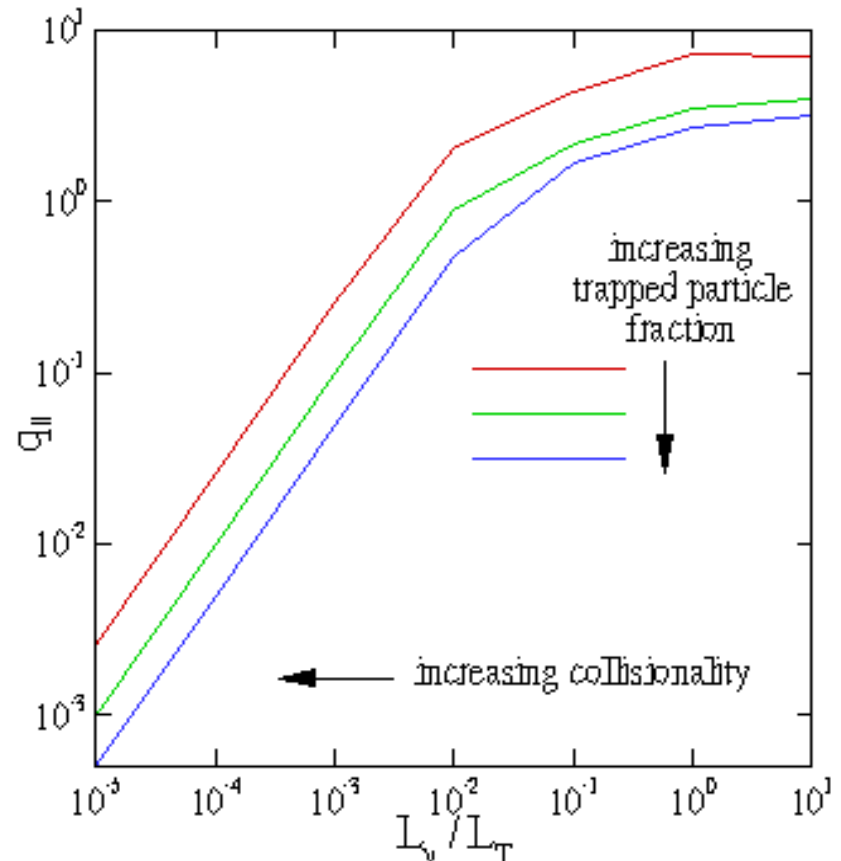
where it is assumed that $\nabla \times (\mathbf{V}_0 \times \mathbf{B}_0 - \eta_0 \mathbf{J}_0) = \mathbf{0}$

- This is fully self-consistent only when the 0-subscripted fields represent a steady state of the entire modeled system.
- If the dynamics of interest are fast relative to any transients from a discrepancy, then the inconsistency is not important.
- Steady-state terms are equivalent to sources in the full system.
- The 0-subscripted fields can be set to zero to model the entire discharge if sources are specified separately.
- This formulation easily allows for true linear computations.

Highlights from Recent Code Development

General, parallel heat flow and stress closures are being implemented in NIMROD. [E. Held, USU]

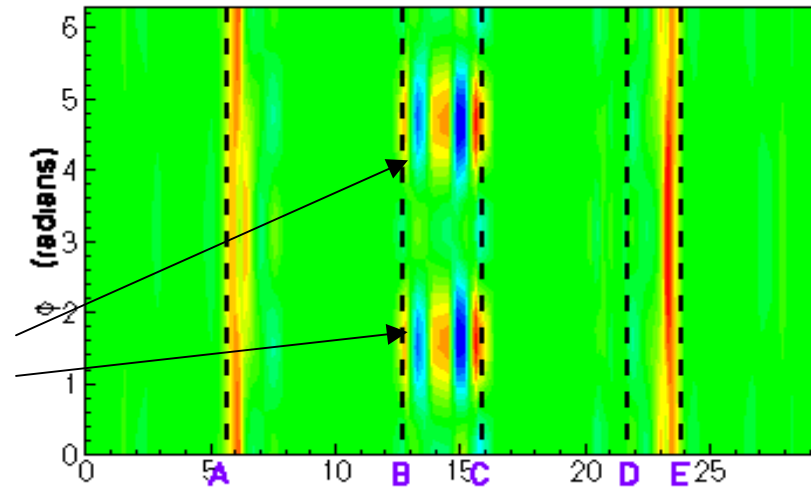
- Heat and momentum transport in high-T, magnetized plasmas depend on q_{\parallel} and Π_{\parallel} closures.
- Derive closures from lowest-order solution to Chapman-Enskog-like (CEL) drift kinetic equation.
- Closures include:
 - (1) quantitative collisional effects with full moment approach of linearized Coulomb collision operator, and
 - (2) free-streaming and particle trapping physics,
 - (3) work underway on derivation of higher-order moment equations for comparison with CEL approach.
- NIMROD's numerical implementation of closures scales to thousands of processors.



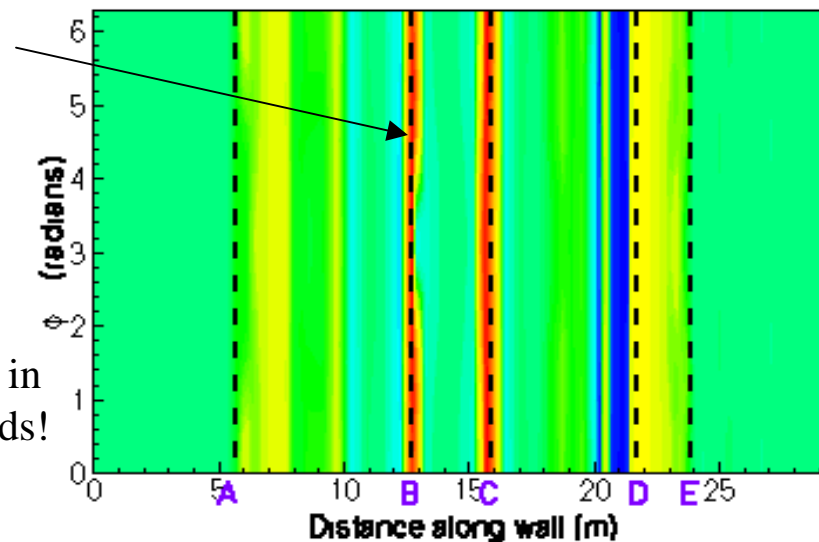
Heat flow response, q_{\parallel} , to T perturbation decreases with increasing collisionality and trapped particle fraction.

General q_{\parallel} is useful for studies of wall heat load during disruption.

Wall heat load using diffusive (Braginskii) closure localized in toroidal angle, ϕ .

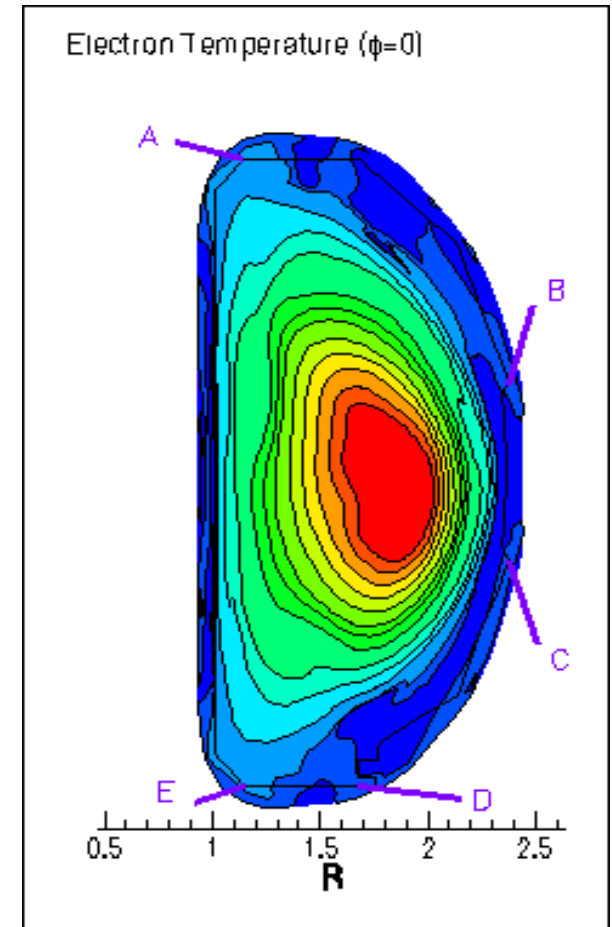


Wall heat load using general closure distributed in toroidal angle, ϕ .



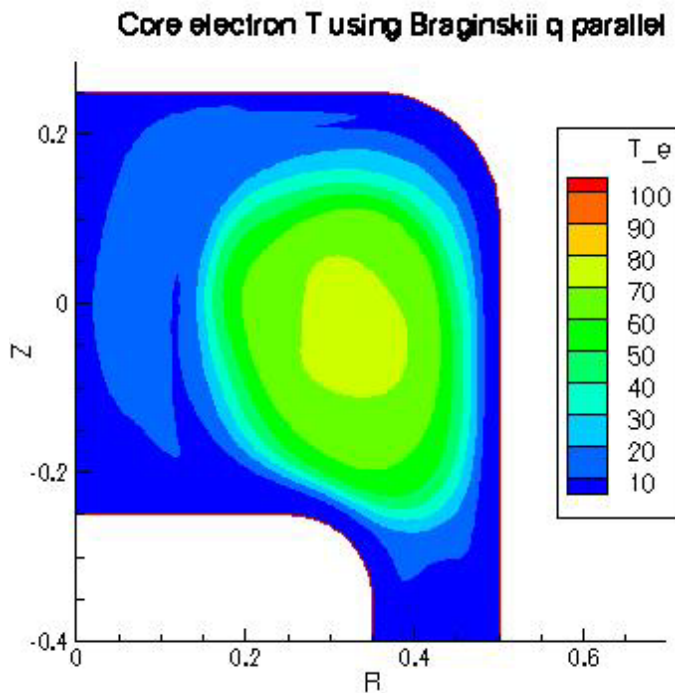
More work needed to understand differences in predicted wall heat loads!
Relevance to ITER.

Electron temperature late in disruption phase. Points along wall shown in heat load plots at left.

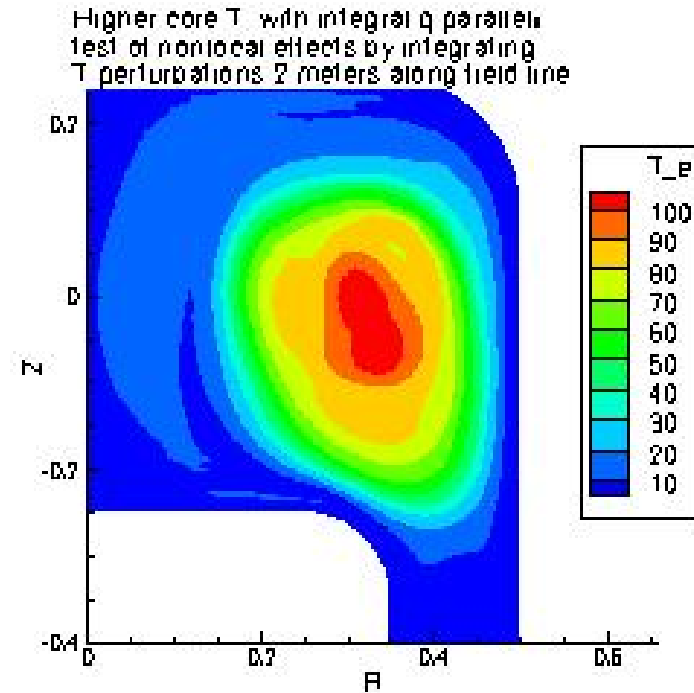


The general closure is also being applied to SSPX. [J.-Y. Ji]

- Our earlier study used Braginskii heat flux with MHD, which reproduces global dynamics and the evolution of magnetic fluctuation levels but over-predicts parallel heat transport along stochastic field-lines.



Collisional Closure

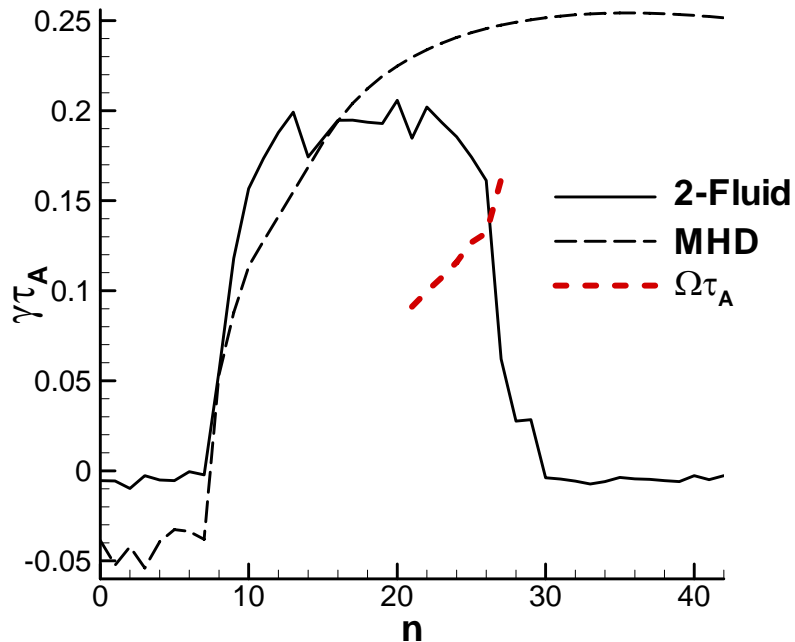


General Closure

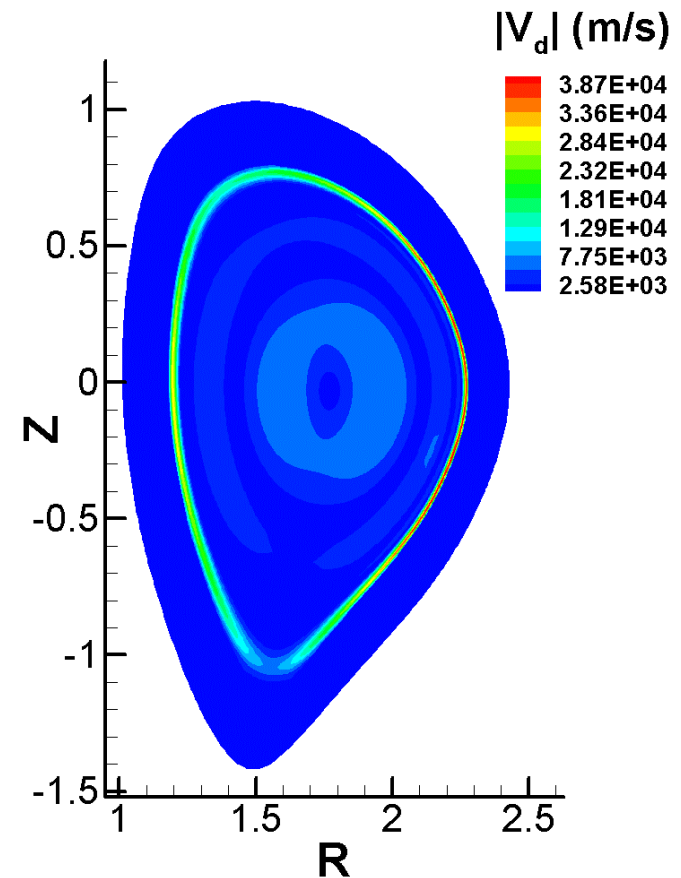
- In a thermal transport computation, the general closure limits heat flux in the core, where temperatures are high and transitions to collisional transport near the walls.
- The USU group is investigating techniques to make the integral evaluations more efficient and to take advantage of increased parallelism.

Recent developments for implicit Hall and gyroviscosity are being applied in production computations.

- Two-fluid cutoff of linear ELM spectrum for DIII-D 113317 equilibrium is confirmed.
- The diamagnetic drift profile is narrower than low-n ELM eigenfunctions.
- Computed stability threshold is at ω_{*i} much greater than $2\gamma_{\text{MHD}}$, which appears to be related to analysis by Ramos, Hastie, and Catto.



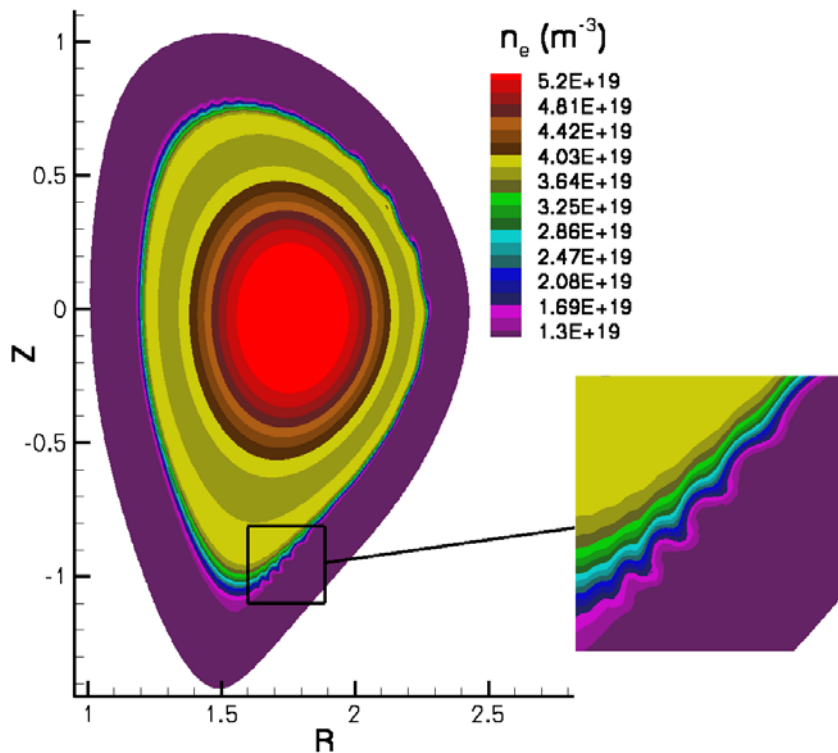
Comparison of resistive MHD and two-fluid growth-rate spectra. Mode frequency is not a simple Doppler shift.



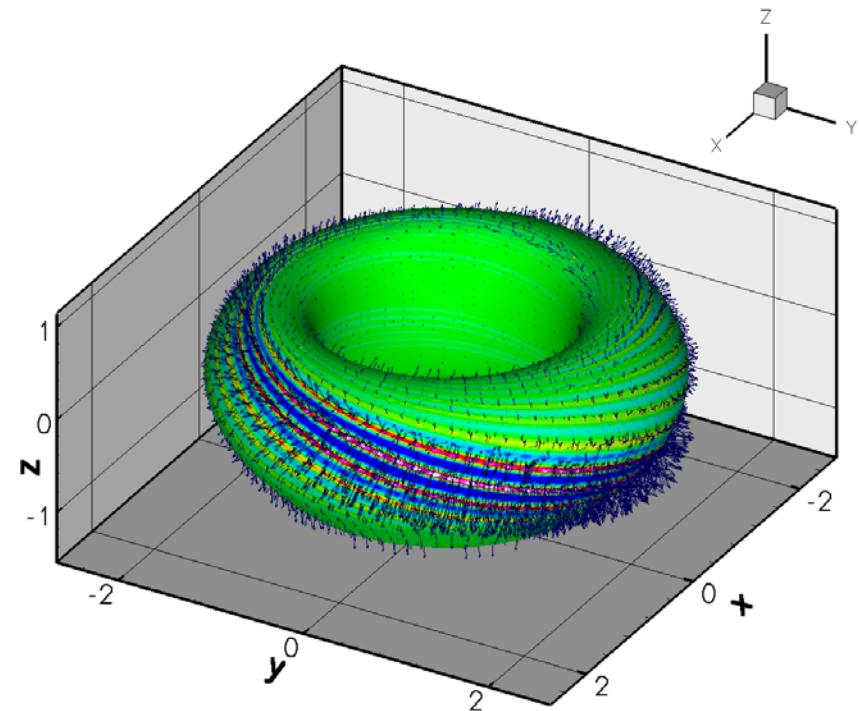
Poloidal component of diamagnetic drift.

The FY2006 milestone computation explored nonlinear two-fluid localization of ELMs in global geometry.

- Project's first large-scale 3D computation with Hall effect and Braginskii gyroviscosity.
- Nonlinear evolution from DIII-D 113317 equilibrium includes toroidal modes $0 \leq n \leq 42$.
- Beating of modes produces helical localization, unlike our previous MHD results.



Number density in the $\phi=0$ plane at simulation shows poloidally localized ripples.



Temperature perturbations reach 100 eV at this time ($T_{ped}=400$ eV) and display a nonlinear helical structure. Perturbed plasma flow vectors are superposed.

Integration with RF for ‘Slow’ MHD

based on draft whitepaper by Hegna, Callen, Schnack, et al.

- NTM is a slow nonlinear instability associated with neoclassical effects from pressure perturbations within magnetic islands.
- Empirical observations of NTMs indicates ρ_i / a scaling for onset, which is unfavorable for ITER .
- Stabilization via RF current drive is expected to be essential and has been proven in present-day tokamaks.
- Comprehensive simulations of ITER need to couple RF and MHD modeling.
- The proposed strategy focuses on ECE stabilization first.
 - First step for the MHD side is to restart NTM modeling and add a prescribed emf.
 - Second step adds a relatively simple model of the interaction, similar to Giruzzi’s, with source information from RF computations.
 - Third step uses D_{ql} from F-P computation in a closure of the fluid equations, using the theoretical framework for the generalized closures.

Discussion

- Providing data for other codes: as a Galerkin computation, all fields are unambiguously defined at all points in the domain.
- Receiving data from other codes: information is needed at the points used for numerical quadrature.
 - Data from other codes can be interpolated, but this may be arbitrary.
 - If information-exchange process is not invertible, there may be loss of accuracy or numerical instability.
- Even the relatively simple RF-coupling problem is interesting.
 - RF-driven currents and evolving MHD \mathbf{B} must be consistent.